MRS Advances (2026) 11:716–723
https://doi.org/10.1557/s43580-026-01550-6

ORIGINAL PAPER

Green synthesis of ZnO nanoparticles using *Passiflora incarnata* extract: Study of structural, morphological, optical, and photocatalytic properties for organic dye degradation

Daniel Perez Villalpando[1] · Aleksy Moreno Meza[1] · Alfredo Rafael Vilchis Nestor[2] · Priscy Alfredo Luque Morales[1]

Received: 30 September 2025 / Accepted: 14 January 2026 / Published online: 30 January 2026
© The Author(s) 2026

Abstract

Zinc oxide (ZnO) nanoparticles were synthesized via a green approach using *Passiflora incarnata* extracts (1, 3, 5%) to evaluate the effect of precursor concentration on their physicochemical and photocatalytic properties. UV–Vis spectroscopy revealed an absorption peak at 367 nm, with bandgap values decreasing from 2.90 to 2.58 eV as the extract concentration increased. XRD confirmed the zincite phase with crystallite sizes of 30.13, 15.68, and 11.55 nm, while FTIR identified phytochemical functional groups and Zn–O stretching. SEM–EDS showed semi-spherical nanoparticles with moderate agglomeration and extract derived organic residues. Photocatalytic degradation of six dyes under UV irradiation for 180 min demonstrated variable efficiencies: enhanced performance for MO (80.67%), AB (92.06%), AY (80%) and MR (73.48%), but reduced activity for RhB (43.25%) and MB (57.04%) at higher extract concentrations. These results highlight the potential of *Passiflora incarnata* mediated ZnO nanoparticles as efficient, ecofriendly photocatalysts for wastewater remediation.

Introduction

Environmental protection, particularly against water pollution, is a global challenge that has driven the search for strategies to treat organic contaminants. Nanotechnology provides innovative solutions, by leveraging the distinctive properties of nanomaterials [1, 2]. Treating wastewater containing dyes has traditionally relied on conventional methods, including physical, chemical, and biological processes [3]. Physical methods include membrane filtration, adsorption and, coagulation [4]. These methods have the advantage of low operating costs and ease of operation [5]. Biological methods use algae, fungi, and enzymes to remove dyes from wastewater through adsorption and biodegradation [6]. Chemical methods include processes such as ozonation and the electro Fenton process [7]. Both of which offer the advantage of being economical [8]. Although these methods have proven effective in different contexts, they still involve the use of large amounts of chemicals, which are not environmentally friendly and are believed to generate toxic byproducts [9]. In this regard, heterogeneous photocatalysis emerges as an alternative for degrading dyes in wastewater. This process is based on the generation of electron–hole pairs (e^-/h^+), which, when a semiconductor is irradiated with light of energy equal to or greater than its bandgap, lead to the formation of reactive oxygen species such as hydroxyl radicals and superoxide [10]. Capable of degrading complex organic compounds. Among the most studied materials are TiO_2 and ZnO, due to their high chemical stability and ability to absorb ultraviolet light [11]. Vasantharaj et al. [12]. Reported the synthesis of zinc oxide nanoparticles using *Ruellia tuberosa*, obtaining rod-shaped nanoparticles with sizes ranging from 40 to 50 nm. They also achieved degradation efficiencies of 94% for methylene blue and 92% for malachite green under UV irradiation. These results demonstrate that the ecological synthesis of zinc oxide nanoparticles using natural extracts is practical for producing nanomaterials with desirable nanoscale properties. On the other hand, Radambabu et al. [13]. Synthesized zinc oxide nanoparticles using *Phoenix dactylifera* pulp. The results

Alfredo Rafael Vilchis Nestor was an editor of this journal during the review and decision stage. For the MRS Advances policy on review and publication of manuscripts authored by editors, please refer to https://mrs.org/editor-manuscripts.

✉ Priscy Alfredo Luque Morales
pluque@uabc.edu.mx

[1] Facultad de Ingeniería, Arquitectura y Diseño, Universidad Autónoma de Baja California, C. P. 22860 Ensenada, Mexico

[2] Centro Conjunto de Investigación en Química Sustentable, UAEM-UNAM, C.P. 50200 Toluca, Mexico

showed a spherical morphology with a size of 30 nm. *Passiflora incarnata L.*, belonging to the family *Passifloraceae*, is one of the most widely used medicinal plants in traditional medicine. Extracts of *P. incarnata* have been reported to exhibit diverse pharmacological activities, including antitussive, analgesic, anticonvulsant, anti-inflammatory, antiasthmatic, anticancer, antimicrobial, antioxidant, and aphrodisiac effects. Its main bioactive constituents, vitexin and isovitexin, are known to modulate gamma-aminobutyric acid type A and B (GABAA_AA and GABAB_BB) receptors and to influence GABA uptake [14, 15]. In this study, zinc oxide nanoparticles were synthesized via green synthesis using *Passiflora incarnata* extract as both a reducing and stabilizing agent, selected for its medicinal properties and novelty. Their photocatalytic performance was evaluated by degrading six organic dyes.

Materials and methods

Materials

The dried leaves of *Passiflora incarnata* were obtained from a local herbalists store. Sigma-Aldrich purchased zinc nitrate hexahydrate, and deionized water was used as the solvent. In addition, six industrial dyes were used: Alizarin Yellow (AY), Methyl Orange (MO), Methylene Blue (MB), Amido Black (AB), Methyl Red (MR), and Rhodamine B (RhB), each at 15 ppm.

Preparation extract

To obtain the active compounds, 0.5, 1.5, and 2.5 g of extract were first weighed. Then, 50 mL of distilled water was added to each sample. The mixtures were stirred for 2 h and then heated in a water bath at 60 °C for 1 h. Finally, the solutions were filtered under vacuum and stored for later use.

Synthesis of ZnO NP

2 g of zinc nitrate hexahydrate were dissolved in Passiflora incarnata extract at 1, 3, and 5% concentrations, stirred for 1 h, and then heated at 60 °C for 12 h to form a paste. The material was thermally treated at 400 °C for 1 h, yielding a grayish-white product that was ground and labeled ZnO/PA-1%, ZnO/PA-3%, and ZnO/PA-5%. These samples were subsequently characterized and tested for photocatalytic activity.

Photocatalytic activity

The study employed six different organic dye solutions: Alizarin Yellow (AY), Methyl Orange (MO), Methylene Blue (MB), Amido Black (AB), Methyl Red (MR), and Rhodamine B (RhB), each at 15 ppm. Degradation experiments were conducted under UV irradiation using 10 W Polaris UV-1 C lamps with an 18 mJ/cm^2 energy output.

Results

UV–Vis and XRD

To determine the optical properties of the zinc oxide nanoparticles, the UV–Vis absorption spectrum was obtained. The characteristic ZnO peak appears at 367 nm (Fig. 1a), confirming the successful formation of the ZnO NPs. To calculate the bandgap, the TAUC model (1) was applied, where α corresponds to the absorption coefficient, $h\nu$ to the photon energy, n to the transition type parameter, A to the material constant, and Eg to the bandgap. Figure 1b–d shows the extrapolated values obtained from the linear portion of the plot. The resulting bandgap energies were 2.90 eV for ZnO/PA–1%, 2.86 eV for ZnO/PA–3%, and 2.58 eV for ZnO/PA–5%, indicating a slight decrease in bandgap with increasing extract concentration. The variations in the bandgap values obtained from the TAUC plots can be attributed to differences in particle size, morphology, and surface states. Changes in crystallite size can produce slight shifts due to quantum confinement. At the same time, defects, surface states, and Urbach tails, often enhanced by organic residues from the plant extract, can modify the apparent absorption edge. Additionally, variations in carrier concentration due to impurities or adsorbed species may result in Burstein Moss type shifts. These factors, widely reported in recent studies on nanostructured ZnO, account for the differences in the calculated bandgaps and underscore the importance of considering structural and surface characteristics when interpreting TAUC plots [16, 17].

$$(\alpha h\nu)^{n} = A(h\nu - Eg) \quad (1)$$

The crystalline structure of the ZnO nanoparticles was analyzed using X-ray diffraction (XRD) (Fig. 1e). The diffraction pattern exhibited distinct peaks at 31.77, 34.42, 36.25, 47.54, 56.60, 62.85, 66.38, 67.95, 69.09, 72.56, and 76.96°, corresponding to the (100), (002), (101), (102), (110), (103), (200), (112), (201), (004), and (202) crystallographic planes of the zincite structure, in agreement with the JCPDS card No. 01–089–7102.

The Debye-Scherrer equation was used to determine the crystalline size (2)

$$D = \frac{K\lambda}{\beta.Cos\theta} \quad (2)$$

where D is the crystallite size (in nm), K known as the Scherrer's constant is a dimensionless constant equal to 0.9,

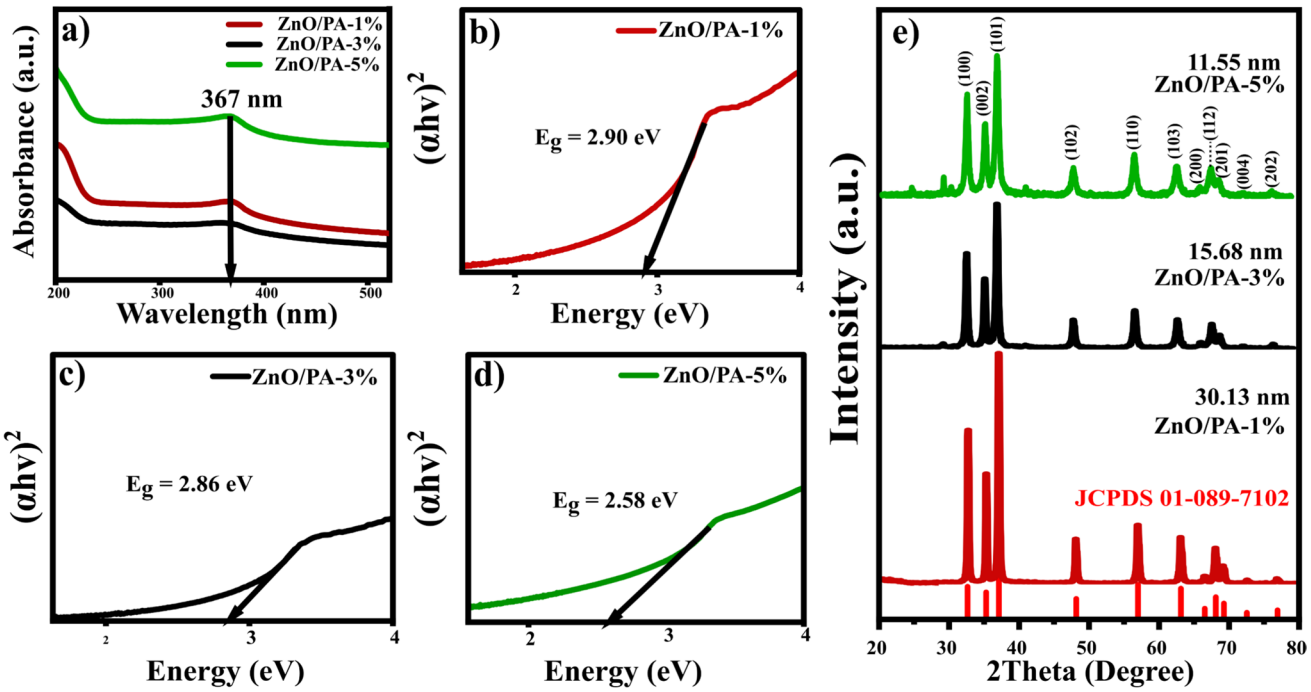


Fig. 1 **a** UV–Vis spectra of ZnO/PA–1%, ZnO/PA–3%, and ZnO/PA–5%, **b** TAUC plot for ZnO/PA–1% **c** TAUC plot for ZnO/PA–3%, **d** TAUC plot for ZnO/PA–5% and, **e** X-ray diffraction (XRD) patterns of ZnO nanoparticles synthesized with *Passiflora incarnata* extract at different concentrations (1, 3, and 5%)

λ corresponds to the incident x-rays wavelength (1.541 Å), β is the full width at half maximum (FWHM) in radians of the main peak of the diffractogram and θ is the Bragg angle of the main peak. The crystallite dimensions (D) correspond to 30.13, 15.68, and 11.55 nm for ZnO/PA-1%, ZnO/PA-3% and ZnO/PA-5% [18]. On the other hand, This small potassium signal may be due to impurities or residual material from the natural extract of *Passiflora incarnata* this assumption is strengthened because the more concentration of *Passiflora incarnata* extract used in the synthesis of ZnO nanoparticles, the Kα signal becomes more prominent [19].

EDS and FTIR

Energy-dispersive X-ray spectroscopy (EDS), shown in Fig. 2a–c, confirms the elemental composition of the synthesized ZnO nanoparticles. The spectra exhibit prominent peaks corresponding to zinc (Zn), oxygen (O), and carbon (C), the latter attributed to residual organic compounds from the plant extract used during synthesis. The increase in carbon and oxygen content with higher extract concentrations reflects a greater presence of organic components, indicating that higher extract concentrations introduce more phytochemicals that act as stabilizing agents. Functional groups were further analyzed using Fourier-transform infrared spectroscopy (FTIR) (Fig. 2d), which revealed characteristic absorption peaks at 3288, 2919, 2849, 1409, 1118, and 869 cm^{-1}, corresponding to O–H, $–CH_3$, $–CH_2$, C–N, C–O, and C–H groups associated with *Passiflora incarnata*. The Zn–O vibration observed at 548 cm^{-1} confirms the successful formation of zinc oxide nanoparticles [20].

Morphology

Figure 3a–c depicts the morphological features of the ZnO nanoparticles (ZnO NPs). The micrographs indicate that the nanoparticles predominantly exhibit a semi-spherical shape with a rough surface texture. Although moderate agglomeration is observed, the nanoparticles are distributed relatively homogeneously across the field of view. This tendency to agglomerate is generally associated with the high surface to volume ratio of nanomaterials, which increases surface energy and enhances van der Waals and electrostatic interactions. A higher number of smaller, well-defined nanoparticles is evident, particularly at higher extract concentrations. This effect is attributed to stabilizing (capping) agents in the *Passiflora incarnata* extract, which limit particle growth and prevent agglomeration by binding to the nanoparticle surfaces [21]. Nevertheless, some residual agglomeration likely persists due to nanoscale ZnO intrinsically high surface energy, which promotes interparticle adhesion and the formation of larger aggregates. The principle of green synthesis is to produce nanomaterials in an environmentally friendly way using natural extracts containing antioxidant molecules,

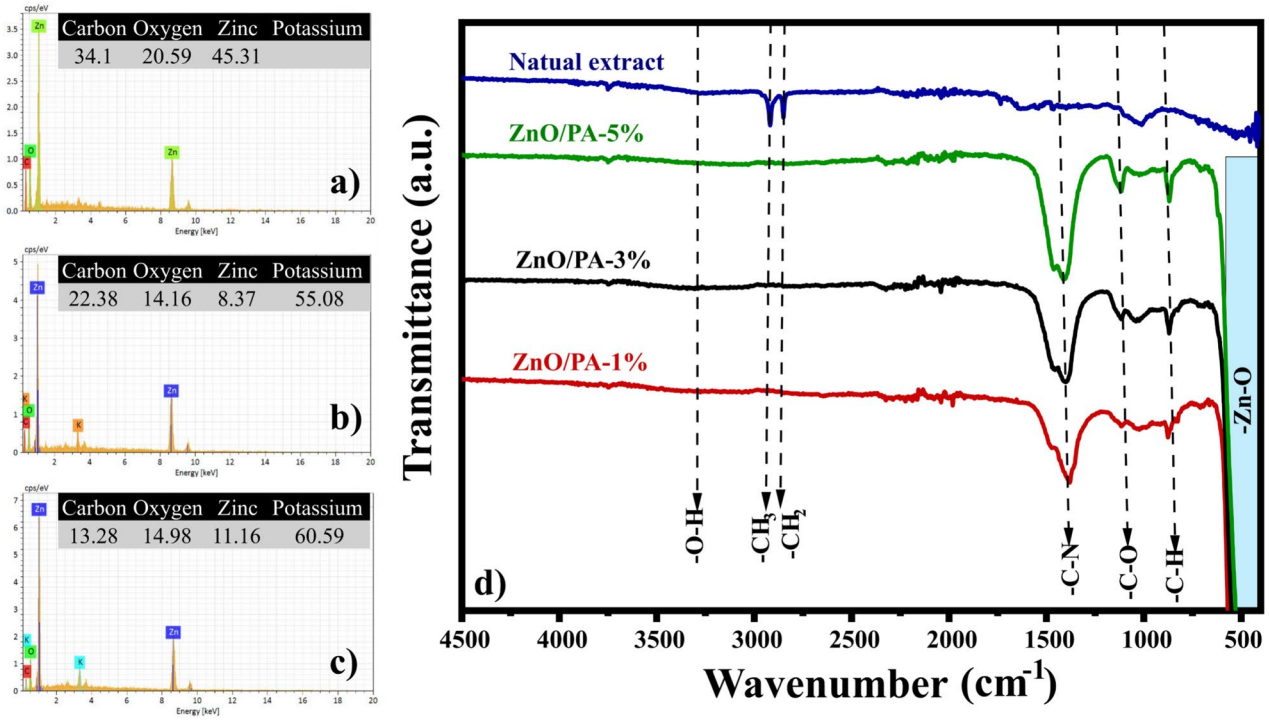


Fig. 2 Elemental composition of ZnO nanoparticles determined by EDS for **a** ZnO/PA-1%, **b** ZnO/PA-3%, **c** ZnO/PA-5%; and **d** Functional group analysis obtained by FTIR

such as flavonoids and polyphenols as seen in Fig. 3d. These bioactive compounds act as reducing and stabilizing agents during nanoparticle formation, so *Passiflora incarnata* can also be used to synthesize metal oxide nanoparticles other than zinc oxide. In fact, plant mediated synthesis of tin oxide and nickel oxide nanoparticles has already been reported [22]. The underlying mechanism is commonly attributed to the complexation of metal ions by phytoconstituents, followed by controlled nucleation and growth during calcination. This process can promote phase purity when reaction conditions are correctly optimized. Therefore, the simple *Passiflora*-based approach described here could be adapted by appropriately adjusting the precursor, pH, temperature, and calcination parameters to synthesize a broader range of metal oxide nanomaterials for catalytic, electronic, and antimicrobial applications [23].

Photocatalytic activity

The photocatalytic performance of the ZnO nanoparticles synthesized using *Passiflora incarnata* extract was systematically evaluated against six organic dyes: Alizarin Yellow (AY), Methyl Orange (MO), Rhodamine B (RhB), Amido Black 10B (AB), Methyl Red (MR), and Methylene Blue (MB) (Fig. 4). For AY, an adsorption–desorption equilibrium was observed during the first 30 min, with ZnO/PA-5% exhibiting the strongest interaction with the dye, whereas ZnO/PA-1% and ZnO/PA-3% showed similar profiles. Under UV irradiation, the degradation efficiencies reached 35.81%, 40.83%, and 50.46% for ZnO/PA-1%, ZnO/PA-3%, and ZnO/PA-5%, respectively. MO displayed minimal initial adsorption but followed a trend similar to AY, achieving efficiencies of 54.66, 56.59, and 80.67% for ZnO/PA-1%, ZnO/PA-3%, and ZnO/PA-5%, respectively [24] In contrast, RhB a cationic and structurally stable dye showed the highest degradation with ZnO/PA-1% (91.29%), while ZnO/PA-3% and ZnO/PA-5% reached only 43.25% and 50.57%, respectively. This inverse behavior is likely associated with excessive extract coating at higher concentrations, which may limit the availability of active sites, partially block UV light, and promote electron–hole recombination. AB followed a positive trend, with degradation efficiencies increasing from 78.32 (ZnO/PA-1%) to 87.24% (ZnO/PA-3%) and 92.06% (ZnO/PA-5%). MR also exhibited enhanced degradation with extract concentration, with efficiencies of 46.10%, 56.62%, and 73.48% for ZnO/PA-1%, ZnO/PA-3%, and ZnO/PA-5%, respectively. Conversely, MB displayed decreasing photocatalytic efficiency with increasing extract content, achieving 74.27%, 69.18%, and 57.04% for ZnO/PA-1%, ZnO/PA-3%, and ZnO/PA-5%, respectively. Overall, these results indicate that, although

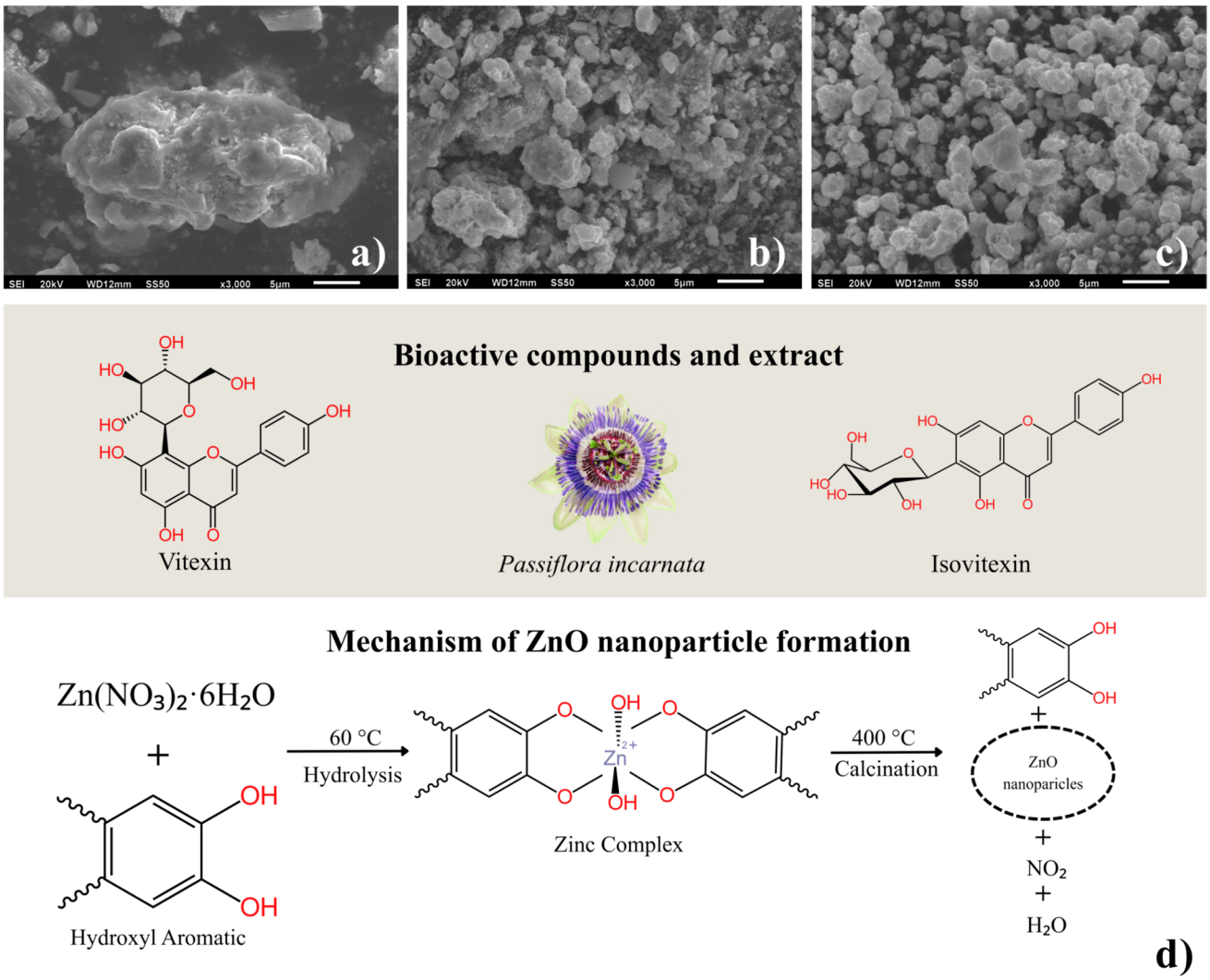


Fig. 3 SEM micrographs of **a** ZnO/PA–1%, **b** ZnO/PA–3%, and **c** ZnO/PA–5%, and **d** proposed mechanism for the formation of zinc oxide nanoparticles using *Passiflora incarnata*

most dyes benefit from higher extract concentrations, cationic or structurally stable dyes such as RhB and MB may exhibit reduced photocatalytic activity due to surface blocking, limited UV penetration, and increased charge recombination. This highlights the importance of optimizing extract concentration depending on the dye class and molecular structure [25]. The proposed photocatalytic mechanism is illustrated in (Fig. 4g). Under continuous UV irradiation, the ZnO nanoparticles generate electron–hole pairs, which subsequently react with adsorbed water and oxygen to form reactive oxygen species (ROS), including hydroxyl radicals (OH) and superoxide anions (O_2^-) [26]. These ROS play a dominant role in dye degradation by attacking and destabilizing the chromophore structures, ultimately leading to molecular breakdown.

Conclusion

In this work, *Passiflora incarnata* extract was successfully employed as a biogenic agent for the green synthesis of ZnO nanoparticles, demonstrating its effectiveness in tailoring the physicochemical properties of the resulting materials. The nanoparticles exhibited a hexagonal zincite structure, with crystallite size decreasing as the extract concentration increased, and presented irregular surface morphologies influenced by the organic constituents of the extract. Optical characterization confirmed the formation of ZnO, while variations in the bandgap were attributed to changes in particle size, surface states, and phytochemical interactions. The photocatalytic evaluation revealed

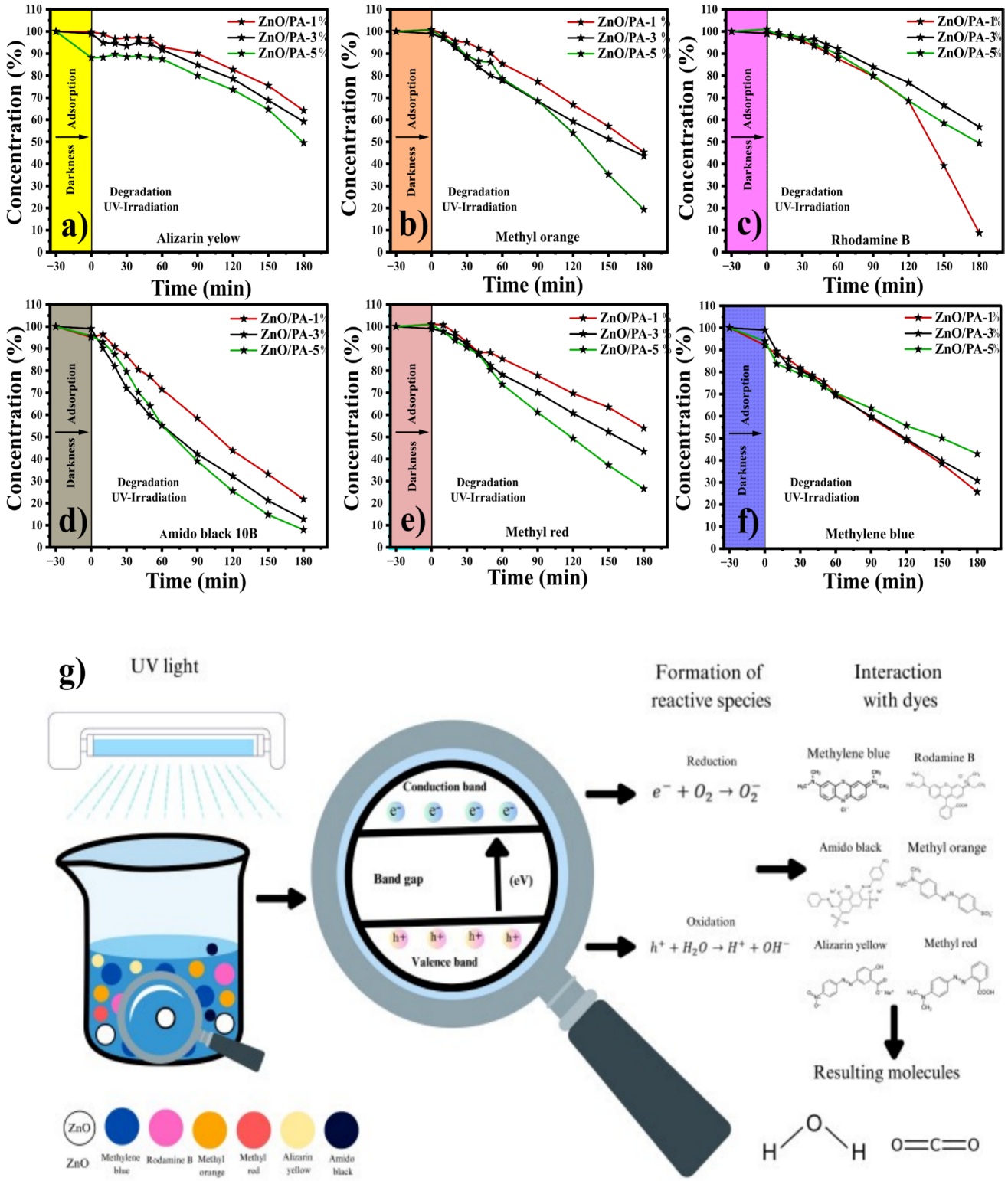


Fig. 4 Photocatalytic degradation of ZnO nanoparticles synthesized using *Passiflora incarnata* extract at concentrations of 1, 3, and 5% against different dyes: **a** AY, **b** MO, **c** RhB, **d** AB, **e** MR, and **f** MR under UV irradiation for 180 min, and **g** proposed reaction mechanism

that all ZnO samples degraded the selected organic dyes under UV irradiation, with performance dependent on both the extract concentration and the dye type. In particular, higher extract contents enhanced degradation for most dyes, although cationic and structurally stable dyes displayed inverse trends, likely due to surface passivation and reduced photon absorption. Overall, these findings highlight the potential of *Passiflora incarnata* assisted synthesis as a sustainable, tunable approach for producing ZnO nanoparticles suitable for photocatalytic and environmental remediation applications.

Acknowledgments The authors would like to acknowledge the support received from projects 402/3391 and 402/3751 at UABC, as well as project 402/1/C/58/24. This research was funded by the Frontera Science Project, grant number CF-2023-I-1805, from CONACYT.

Author contributions Daniel Perez Villalpando: methodology, investigation, visualization, writing original draft. Aleksy Moreno Meza: conceptualization, investigation. Alfredo Rafael Vilchis Nestor: visualization, data curation, writing original draft. and Priscy Alfredo Luque Morales: methodology, investigation, visualization, writing original draft.

Funding This work was funded by conacyt, CF-2023-I-1805, Alfredo Luque.

Data availability The data may be available upon request from the author.

Declarations

Conflict of interest The author declares that there are no conflicts of interest.

Open Access This article is licensed under a Creative Commons Attribution 4.0 International License, which permits use, sharing, adaptation, distribution and reproduction in any medium or format, as long as you give appropriate credit to the original author(s) and the source, provide a link to the Creative Commons licence, and indicate if changes were made. The images or other third party material in this article are included in the article's Creative Commons licence, unless indicated otherwise in a credit line to the material. If material is not included in the article's Creative Commons licence and your intended use is not permitted by statutory regulation or exceeds the permitted use, you will need to obtain permission directly from the copyright holder. To view a copy of this licence, visit http://creativecommons.org/licenses/by/4.0/.

References

1. P. Emerson, M. Jothibas, P.A. David, Eco-sustainable synthesis of α-Fe_2O_3/rGO nanocomposite and their interfacial effect towards on visible light photocatalysis. Inorg. Chem. Commun. **176**, 114317 (2025)
2. R. Saini, P. Kumar, Green synthesis of TiO_2 nanoparticles using *Tinospora cordifolia* plant extract & its potential application for photocatalysis and antibacterial activity. Inorg. Chem. Commun. **156**, 111221 (2023)
3. M. Tabish, A.B. Tabinda, Z. Mazhar, A. Yasar, J. Ansar, I. Wasif, Physical, chemical and biological treatment of textile wastewater for removal of dyes and heavy metals. Desalin. Water Treat. **320**, 100842 (2024)
4. H.M. Solayman, Performance evaluation of dye wastewater treatment technologies: a review. J. Environ. Chem. Eng. **11**(3), 109610 (2023)
5. M.A. Zayed, Z.A. Abo-Ayad, S.S. Medany, Catalytic efficient electro-oxidation degradation of DO26 textile dye via UV/VIS, COD, and GC/MS evaluation of by-products. Electrocatalysis **12**(6), 731–746 (2021)
6. A. Singh, Biological remediation technologies for dyes and heavy metals in wastewater treatment: new insight. Bioresour. Technol. **343**, 126154 (2022)
7. G. Bal, A. Thakur, Distinct approaches of removal of dyes from wastewater: a review. Mater. Today Proc. **50**, 1575–1579 (2022)
8. A. Ahmadi Zahrani, B. Ayati, Using heterogeneous Fe-ZSM-5 nanocatalyst to improve the electro fenton process for acid blue 25 removal in a novel reactor with orbiting electrodes. J. Electroanal. Chem. **873**, 114456 (2020)
9. L. Bilińska, M. Gmurek, Novel trends in aops for textile wastewater treatment. Enhanced dye by-products removal by catalytic and synergistic actions. Water Resour. Ind. **26**, 100160 (2021)
10. M.A. Albo Hay Allah, H.K. Ibrahim, H.A. Alshamsi, H. Radhi Saud, Eco-friendly synthesis of biochar supported with zinc oxide as a heterogeneous catalyst for photocatalytic decontamination of rhodamine B under sunlight illumination. J. Photochem. Photobiol. Chem. **449**, 115413 (2024)
11. L. ManikanikaChopra, Photocatalytic activity of zinc oxide for dye and drug degradation: A review. Mater. Today Proc. **52**, 1653–1656 (2022)
12. S. Vasantharaj, Enhanced photocatalytic degradation of water pollutants using bio-green synthesis of zinc oxide nanoparticles (ZnO NPs). J. Environ. Chem. Eng. **9**(4), 105772 (2021)
13. K. Rambabu, G. Bharath, F. Banat, P.L. Show, Green synthesis of zinc oxide nanoparticles using *Phoenix dactylifera* waste as bioreductant for effective dye degradation and antibacterial performance in wastewater treatment. J. Hazard. Mater. **402**, 123560 (2021)
14. F. Suciu, Evaluation of the antihyperalgesic potential of *Morus alba*, *Angelica archangelica*, *Valeriana officinalis*, and *Passiflora incarnata* in alloxan-induced diabetic neuropathy in rats. Curr. Issues Mol. Biol. **47**(9), 719 (2025)
15. K. Elghobashy, M. Eldanasoury, A. Elhadary, D.-M. Farid, Phytochemical constituent, HPLC profiling and antioxidant activity of *Passiflora incarnata* and *Arctium lappa* leaves extracts. Int. J. Vet. Sci. **9**(1), 42–49 (2020)
16. A. Singh, A. Gupta, B. Prasad, K. Ghai, S. Dwivedi, A facile green synthesis of bismuth oxide nanoparticles (BiONPs) mediated through bark extract of Moringa Oleifera lam. and characterization. Discover Chemistry **2**(1), 201 (2025)
17. M.E. Elsisi, M.M. Mostafa, H. Abdella, A.E. Khalil, A.S. Soror, In-depth investigation the size effect of zinc oxide nanostructures on the photodegradation of different dyes under UV-irradiation: anticancer application. Sci. Rep. **15**(1), 31669 (2025)
18. M. Malpani, K. Shekhawat, S. Chattopadhyay, R.D.K. Misra, K.P. Misra, Defects induced photoluminescence and alteration of band gap and morphology in Ca doped sol-gel co-precipitated ZnO nanoparticles. Discov. Appl. Sci. **7**(11), 1303 (2025)
19. M.A. Irshad, Efficient chromium removal from leather industrial wastewater in batch experimental study: green synthesis and characterization of zinc oxide nanoparticles using *Ficus benghalensis* extracts. Ecotoxicol. Environ. Saf. **281**, 116616 (2024)
20. Y. Cao, H.Q. Alijani, M. Khatami, F. Bagheri-Baravati, S. Iravani, F. Sharifi, K-doped ZnO nanostructures: biosynthesis and parasiticidal application. J. Mater. Res. Technol. **15**, 5445–5451 (2021)

21. Z. Villagran, Plant-based extracts as reducing, capping, and stabilizing agents for the green synthesis of inorganic nanoparticles. Resources **13**(6), 70 (2024)
22. A. El Golli, S. Contreras, C. Dridi, Bio-synthesized ZnO nanoparticles and sunlight-driven photocatalysis for environmentally-friendly and sustainable route of synthetic petroleum refinery wastewater treatment. Sci. Rep. **13**(1), 20809 (2023)
23. A.R.N. Aina, H. Patel, S. Aich, B. Roy, N.S. Samanta, B. Pal, Recent advances in ZnO based photocatalysts for industrial dye degradation. Discov. Appl. Sci. **7**(9), 977 (2025)
24. A.M. El-Khawaja, Green synthesized ZnO nanoparticles by *Saccharomyces cerevisiae* and their antibacterial activity and photocatalytic degradation. Biomass Convers. Biorefinery. **15**(2), 2673–2684 (2025)
25. O.H. Sahib, L.Z. Mohammed, M.A. Mahdi, Biosynthesis of copper nanoparticles using *Passiflora* flower extract and study their antimicrobial, antioxidant and anticancer activity. Asian Pac. J. Cancer Prev. **26**(8), 2953–2963 (2025)
26. C.A. Magaña-Chavez, J.A. Villegas-Fuentes, O.J. Nava, A.R. Vilchis-Nestor, P.A. Luque, Green synthesis of semiconductor nanoparticles (ZnO, CuO, and SnO_2) using *Physalis philadelphica* peel extract: characterization and photocatalytic studies on five organic dyes. J. Mater. Sci. Mater. Electron. **36**(26), 1728 (2025)

Publisher's Note Springer Nature remains neutral with regard to jurisdictional claims in published maps and institutional affiliations.